

Volcanological features and preliminary geophysical investigations on Marion Island

L Chevallier* & W J Verwoerd

Department of Geology, University of Stellenbosch, Stellenbosch 7600

P Bova

Geological Survey, PO Box 572, Bellville 7535

E Stettler, A du Plessis, J G du Plessis, L M Fernandez & M Nel

Geological Survey, Private Bag X112, Pretoria 0001

* Current address: Geological Survey, PO Box 572, Bellville 7535

Volcanological features indicate that Marion Island is active but has had a very low eruptive rate during the last 10 000 years. Nearly all Holocene activity occurred along radial fractures. An elongated north-east trending rift zone of maximum activity can be delineated in the south-western sector of the island. The radial fractures and rift zone will probably control future eruptions, which may be expected to be of either hawaiian, strombolian or phreatomagmatic type.

Geophysical investigations of a preliminary nature correlate well with these geological observations. A negative gravity anomaly coincides with the rift zone and may represent a magma chamber at a depth of 3 to 5 km below surface. Seismic recordings during a four-year period (1987 to 1991) detected only four minor events of local origin. These are ascribed to deep magma movements or elastic readjustments. The volcano thus appears not to have a very active shallow plumbing system. Ground magnetic profiles showed a different response between Pleistocene and Holocene lava flows and a distinct signature over dyke-intruded fractures.

Future geophysical work should include gravity observations at sea, routine seismological recordings and an aeromagnetic survey of Marion Island.

Vulkanologiese kenmerke toon dat Marion-eiland aktief is, maar dat die erupsietempo gedurende die afgelope 10 000 jaar baie laag was. Feitlik alle Holoseen-aktiwiteit het langs sekere radiale splete plaasgevind. 'n Sone van maksimum aktiwiteit wat in 'n noordoostelike rigting verleng is kan in die suidwestelike hoek van die eiland afgebaken word. Die radiale splete en aktiewe sone sal waarskynlik toekomstige erupsies kontroleer, wat vermoedelik van die hawaiiese, stromboliese of freatomagmatiese tipe sal wees.

Geofisiese ondersoeke van 'n voorlopige aard bevestig hierdie geologiese afleidings. 'n Negatiewe gravitasieanomalie val saam met die aktiewe sone en mag dalk 'n magmakamer op 3 tot 4 km diepte onder die twee vulkaniese sentra verteenwoordig. Seismiese opnames gedurende 'n vier-jaar-toetsperiode (1987 tot 1991) het net vier gebeurtenisse van plaaslike oorsprong aan die lig gebring. Hulle kan toegeskryf word aan diep magma-bewegings of elastiese heraanpassings. Die vulkaan skyn dus in 'n rusperiode te wees.

Magnetometriese profiele op land het verskille tussen die Pleistoseen- en Holoseen-lawavloeiings getoon, asook 'n duidelike sinjatuur vir gange wat langs splete ingedring het.

Toekomstige geofisiese werk behoort gravitasiewaarnemings ter see, roetine-seismologiese registrering en 'n lugmagnetiese opname van Marion-eiland in te sluit.

Introduction

The first geological investigation of Marion Island (Verwoerd 1971), revealed youthful volcanological features indicating that the volcano, although at that time without historical eruptions, was still active. This was confirmed by a fissural eruption on the western flank of the edifice in 1980 (Verwoerd *et al* 1981). As a result, further geological work was carried out by the first author from 1983 to 1987 in order to investigate in detail the history and age of the volcano, the petrology of its lavas, its various eruptive styles and its general past and present behaviour. This was complemented by a reconnaissance geophysical programme utilising gravity, seismic and geomagnetic techniques between 1987 and 1990, in collaboration with the Geological Survey of South Africa. The overall purpose was to bring further constraints on the current model of the internal structure and the predicted behaviour of the volcano.

Previous solid earth geophysical observations on the island consist of gravity-readings near the meteorological station (Wiid 1961) and geomagnetic field variations (Wiid & Van Wyk 1961). A comprehensive geophysical investigation of a volcano involves substantial manpower and a variety of geophysical equipment and disciplines that were beyond the scope of the project. In addition, an accurate topographic base map was not available. The present investigation is therefore preliminary in nature.

The volcanological framework

Marion Island is a shield volcano with slopes that do not exceed 8°. It reaches an elevation of 1 240 m and has a permanent but small ice cap extending down to 1 100 m. Verwoerd (1971) recognised and mapped two main phases of volcanic activity: a Pleistocene one and a Holocene

one, separated by the last glacial event that occurred between 50 000 and 10 000 years ago. The Pleistocene lavas have been dated from older than 450 000 years to 50 000 years. During this interval various building periods have been recognised (Chevallier *et al* in prep, Verwoerd 1990). The stratigraphic analysis specially reveals two distinct series, East and West, and leads to the proposal of two distinct plumbing systems under Marion.

A structural study of the Holocene phase shows that nearly all the eruptions occurred along persistent radial fissures. Most of these fractures are located along or follow the rims of graben-like structures and converge on two distinct volcanic centres located 4 km apart probably related to the two plumbing systems mentioned above (Fig 2, Chevallier 1986). Among these fracture systems three appear to have been more active. The most important one is a fracture zone that runs from the south-western tip of the island up to the north-eastern coast, passing through the two volcanic centres. Most of the recent eruptions took place along this rift. Two other active systems are (1) an E-W fault on the western centre and along which the 1980 fissure eruption occurred, and (2) a SE-NW fault on the south-eastern side of the island.

The Holocene phase produced some 150 volcanic vents and associated flows during the last 10 000 years (Fig 1). Holocene eruptions were mainly of strombolian type: cinder cones up to 200 m high were built up and lava flows of aa or, less commonly, pahoehoe type poured

out. A few eruptions of hawaiian type with spatter cones or ramparts and short flows occurred as well, the latest example being the 1980 eruption. A third type of eruptive style is phreatomagmatic. It has occurred on shallow submerged coastal plains producing typical surtseyan cones (Verwoerd & Chevallier 1987).

The time-average eruptive rate of Marion volcano appears to be very low: 150 eruptions during the last 10 000 years, i.e. an average of one or two eruptions per century. This has continued to the present, with only one eruption in recorded history. Based on various criteria (relative age, degradation of cones, vegetation cover, sediment and palaeosol deposits, palaeobeaches) the Holocene lava flows have been grouped into three main periods of activity. The most recent period corresponds to a group of vents and flows that all show very fresh morphology, rudimentary vegetation growth, and in addition have the same petrological composition (Fig 2). They were either hawaiian eruptions with a small amount of extruded lava (like the 1980 eruption) or strombolian eruptions with a much bigger volume of lava emitted (like the West Peak flow. See Fig 2).

A distribution map of volcanic vents shows that three concentration zones can be distinguished (Fig 3). The first corresponds to the SW-NE rift zone, including the two eruptive centres. In this zone fissures and cones are very closely spaced, within 100 m of each other and often overlapping. The second zone is less densely populated

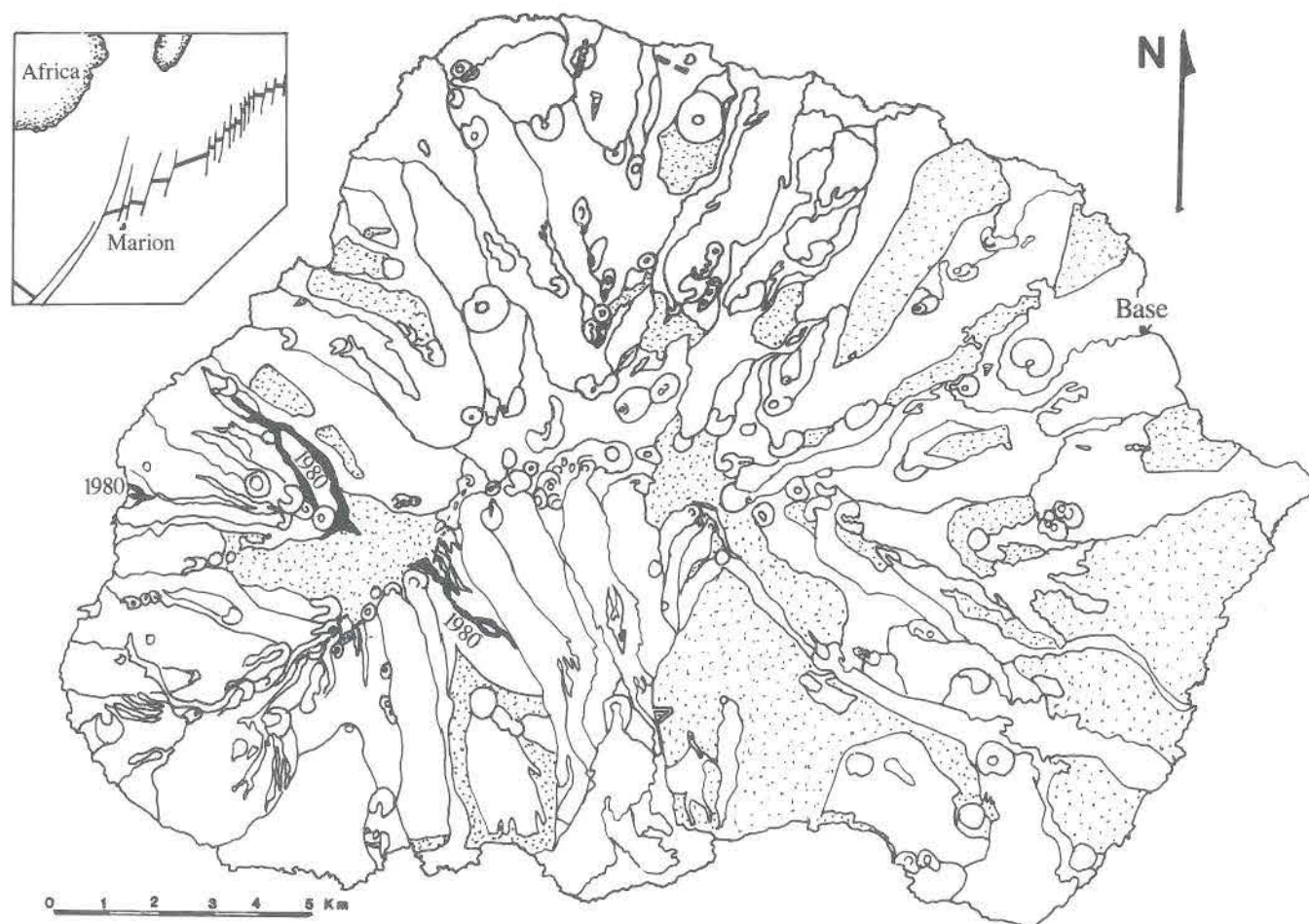


Fig 1: Geological map of Marion Island modified after Verwoerd, 1981. Dotted areas: Pleistocene lavas, blank areas: Holocene lavas with flow boundaries and eruptive vents. The flows of the 1980 eruption are in black

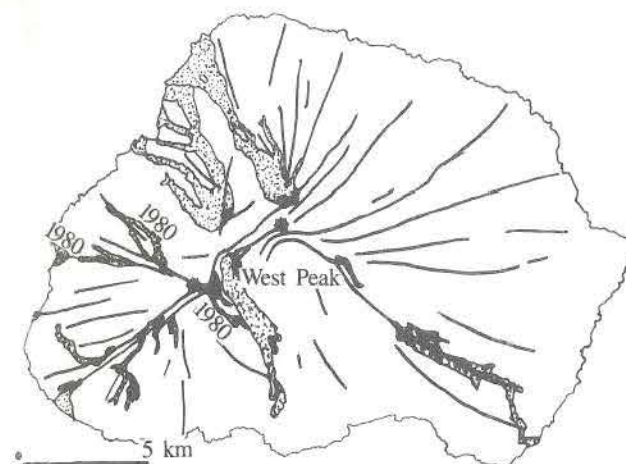


Fig 2: Tectonic map of the Holocene phase. Certain specific radial faults acted as feeding channels. They converge on two eruptive centres (stars). Dotted flows are the most recent Holocene eruptions including that of 1980

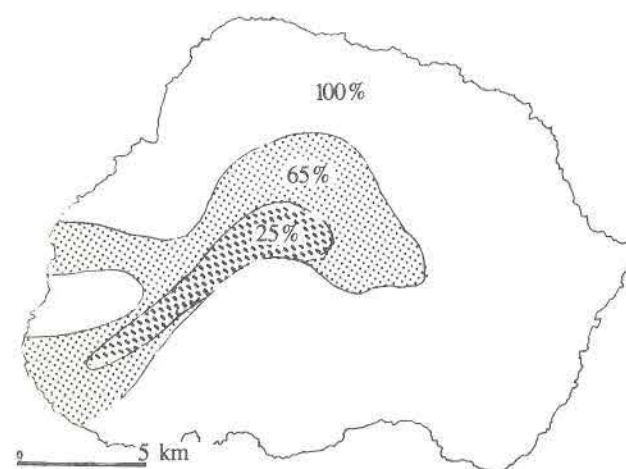


Fig 3: Frequency distribution of Holocene volcanic vents. 25% of the vents are located at the top of the volcano and along the southwestern rift system where they are closely spaced. Note that most of the recent eruptions fall within the 65% area (which includes the 25% area)

but still corresponds to a high degree of activity. It roughly surrounds the highest-concentration zone and in addition has an E-W spur that was the location of the 1980 eruption. In the third zone the eruptive vents are rare, averaging 2 km apart, and this comprises the remainder of the island. Most of the recent Holocene eruptions originated in the first and second zones and only one or two occurred in the third zone (compare Figs 2 and 3). Zones 1 and 2 thus give an approximate delimitation of the most active part of the volcano. The region around the Western centre also seems to have been more active than the Eastern centre during recent Holocene time.

Using stress analysis, rock mechanics and numerical modelling (Chevallier & Verwoerd 1988), a shallow magma chamber, some 3 to 5 km deep, has been postulated for the eruptive phenomena observed on Marion. Whether the two volcanic centres correspond to distinct shallow plumbing systems or whether the magma chamber is a single elongated body cannot be ascertained.

The petrology of the Holocene lavas shows two dis-

tinct types of basalt: a porphyritic olivine + pyroxene + feldspar basalt and a microporphyritic olivine + feldspar basalt. The second type is more evolved than the first one (Verwoerd 1990). All the eruptions of the most recent Holocene period (Fig 2) (except the one at the extreme south-west end of the island) belong to the evolved group. Chevallier and Verwoerd (in prep) conclude that the magma in the chamber has been undergoing a period of differentiation during the last thousand years with almost no permanent replenishment by more primitive magma.

In conclusion the volcanological model of Marion Island could be described as follows:

- There is probably a double or elongated single shallow magma chamber (3 to 5 km) below the volcano that feeds two volcanic centres.
- The rate of eruption during the Holocene period and recent time is very low — only a few eruptions per century.
- The sites of eruptions are determined by persistent radial fractures some of which are very prominent and should be taken into account in any volcanic hazard assessment.

Regional gravity survey

Gravimetry is well suited to volcanology because there are often features that show differences in density under volcanoes (Rymer & Brown 1986), e.g. chambers of crystallised or partly molten magma, dyke networks, zones of unconsolidated volcanic products, caldera infillings. The purpose of the gravimetric observations on Marion was therefore to detect the presence of any distinct structures that could be related to surface features.

Data collection and correction

Forty seven gravity readings were taken on the island with two calibrated LaCoste & Romberg geodetic gravimeters, nos G312 and G314 (Fig 4). A gravity base station, MARO, was tied in from the new first order base station situated at the Surveys and Mapping branch offices at Mowbray, Cape Town. The base station MARO was observed as often as possible, usually before and after the day's work.

All the elevations were determined with two Fuess micro barometers with similar pressure response characteristics. Barometer readings at the meteorological station were used to calculate the drifts of the field barometers. Because of rapid changes in weather conditions, the assumption of linear drift and the fact that the meteorological station is certainly not representative of the whole island, a maximum time-lapse of two hours was allowed between the field and the station barometer readings. In addition, readings were taken at points with known altitude. Helicopter transport was provided to all remote localities within a reasonable time and to protect instruments against damage. Three expeditions were necessary to accomplish the programme: April 1987, August 1987 and August 1988. Technical details have been given by Du Plessis and Bova (1989). The barometric equation (Sears *et al* 1976) was used to calculate the elevations.

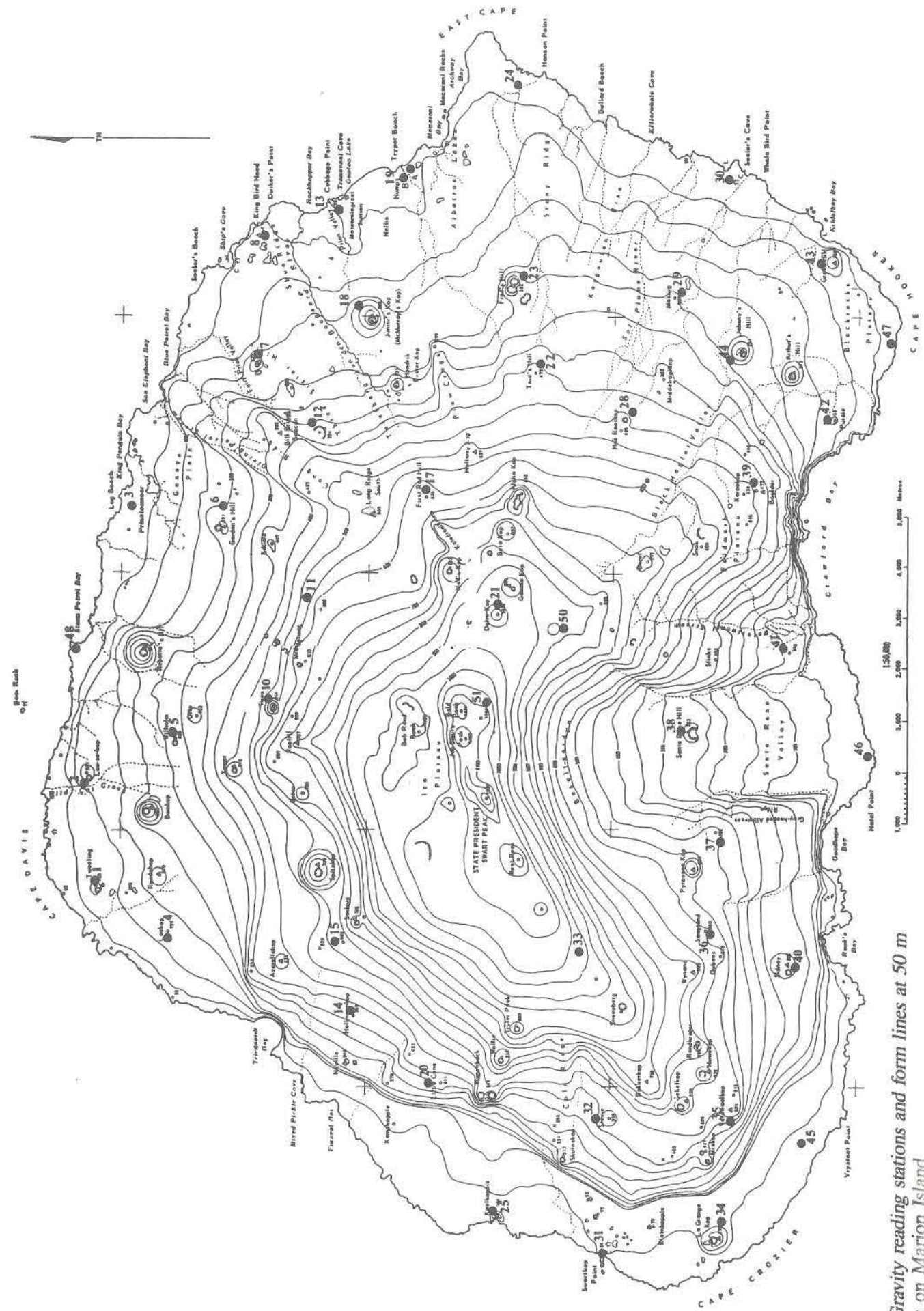


Fig 4: Gravity reading stations and form lines at 50 m intervals on Marion Island

Table 1

Station No	Lat (o)	Lon (o)	Elev (m)	"G"	B Anomaly			Date	Gravim.
					D=2.67	D=2.9	D=2.5		
4637MI001	46.8325	37.6883	51.	980952.16	177.34	176.82	177.60	870501	G312
4637MI002	46.8304	37.7131	110.	980947.50	184.48	183.36	185.21	870501	G312
4637MI003	46.8394	37.7838	16.	980995.55	213.22	213.06	213.32	870429	G312
4637MI004	46.8461	37.6736	96.	980938.74	171.55	170.57	172.18	870501	G312
4637MI005	46.8472	37.7255	347.	980899.99	182.09	178.56	184.39	870814	G134
4637MI006	46.8561	37.7836	105.	980976.36	210.03	208.97	210.73	870429	G312
4637MI007	46.8623	37.8220	102.	980981.34	213.86	212.83	214.54	880831	G134
4637MI008	46.8628	37.8525	24.	981002.67	219.80	219.55	219.96	870418	G132
4637MI010	46.8645	37.7348	566.	980854.75	178.39	172.63	182.13	870814	G134
4637MI011	46.8714	37.7603	456.	980887.36	188.73	184.08	191.74	870823	G134
4637MI012	46.8715	37.8051	266.	980949.85	205.94	203.64	207.44	880831	G134
4637MI013	46.8762	37.8596	29.	981004.46	221.36	221.07	221.55	870418	G312
4637MI014	46.8800	37.6550	351.	980886.11	166.04	162.46	168.36	870502	G312
4637MI015	46.8769	37.6729	519.	980853.03	166.30	161.01	169.73	870502	G312
4637MI017	46.8925	37.7881	620.	980850.00	181.74	175.42	185.84	870816	G134
4637MI018	46.8798	37.8347	132.	980973.00	209.84	208.50	210.72	870419	G312
4637MI019A	46.8892	37.8697	22.	981009.34	223.69	223.47	223.84	870420	G312
4637MI020	46.8948	37.6369	348.	980892.40	170.40	166.86	172.70	870824	G134
4637MI021	46.9062	37.7592	1005.	980775.30	181.56	191.44	188.22	870816	G134
4637MI022	46.9139	37.8201	280.	980938.16	201.05	198.20	202.90	880904	G134
4637MI023	46.9105	37.8423	195.	980960.61	228.89	205.10	208.37	870507	G312
4637MI024	46.9090	37.8912	13.	981009.42	220.21	220.08	220.30	870420	G312
4637MI025	46.9065	37.6043	47.	980950.04	167.75	167.27	168.06	870503	G312
4637IM028	46.9305	37.8082	355.	980923.78	199.93	196.32	202.28	870507	G312
4637IM029	46.9395	37.8387	208.	980958.51	204.92	202.80	206.30	870507	G312
4637IM030	46.9485	37.8681	32.	981007.87	218.83	218.50	219.04	870424	G312
4637IM031	46.9265	37.5932	34.	980951.85	165.19	164.85	165.42	870503	G312
4637IM032	46.9249	37.6279	362.	980883.97	162.01	158.32	164.40	870504	G312
4637IM033	46.9217	37.6705	1022.	980745.77	153.99	143.58	160.74	870816	G134
4637IM034	46.9481	37.6012	113.	980941.01	167.95	166.80	168.70	870504	G312
4637IM035	46.9496	37.6268	468.	980858.71	155.37	150.61	158.47	870814	G134
4637IM036	46.9456	37.6754	452.	980877.41	171.29	166.69	174.28	870505	G312
4637IM037	46.9473	37.6985	409.	980891.34	176.60	172.44	179.61	870505	G312
4637IM038	46.9405	37.7272	242.	980933.67	186.68	184.22	188.28	870505	G312
4637IM039	46.9535	37.7901	468.	980887.40	183.71	178.95	186.81	870506	G312
4637IM040	46.9609	37.6668	244.	980916.15	167.72	165.23	169.33	870505	G312
4637IM041	46.9596	37.7480	152.	980949.75	183.32	181.78	184.33	870505	G312
4637IM042	46.9667	37.8065	97.	980972.69	194.80	193.81	195.44	870424	G312
4637IM043	46.9655	37.8466	13.	980987.79	193.48	193.34	193.56	870424	G312
4637IM044	46.9488	37.8217	239.	980948.91	200.58	198.15	202.16	870506	G312
4637IM045	46.9630	37.6216	67.	980952.70	169.24	168.56	169.68	870814	G134
4637IM046	46.9745	37.7208	12.	980974.12	178.80	170.67	178.88	880901	G134
4637IM047	46.9784	37.8260	21.	980996.94	203.03	202.82	203.17	880901	G134
4637IM048	46.8293	37.7468	161.	980975.63	222.74	221.11	223.81	870823	G134
4637IM050	46.9191	37.7530	850.	980793.35	167.95	159.29	173.57	870816	G134
4637IM051	46.9049	37.7341	1070.	980741.08	160.26	149.26	167.33	870816	G134

The gravimetric data were corrected for instrument drift, tidal variation, estimate of error in readings, elevation, latitude and density (Du Plessis & Bova 1989). No terrain corrections were made. Table 1 gives the Bouguer anomaly values for three density assumptions: 2.5, 2.67 and 2.9. An absolute value for the base station MARO was calculated as described by Du Plessis (1984). The value is 981001,22 + 0,06 mgal.

Results

The reduced gravity data for the 2.67 density assumption are presented in the form of a Bouguer anomaly contour map (Fig 5). Table 1 shows that if the density assumption does influence the Bouguer anomaly maps the three different densities would be similar with a maximum error of 17 mgal (10%) for the two extreme densities at the top of the volcano and a mean error of 6 mgal

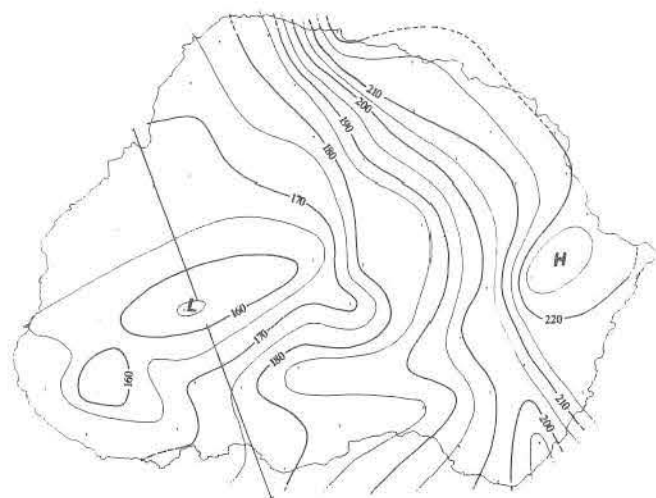


Fig 5: Bouguer anomaly map of Marion Island for density assumption of 2.67 g/cm^3 . Contours in mgal. Note the low gravity values above the most active part of the volcano (cf Fig 3) and the increase towards the east. The localised high anomaly on the east coast needs reconfirmation

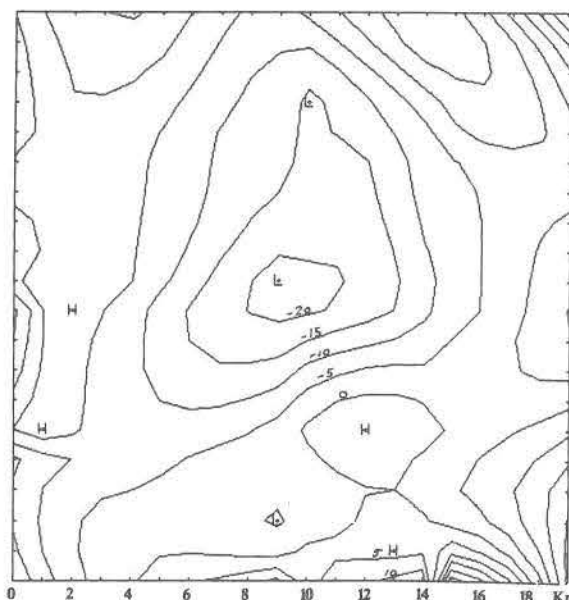
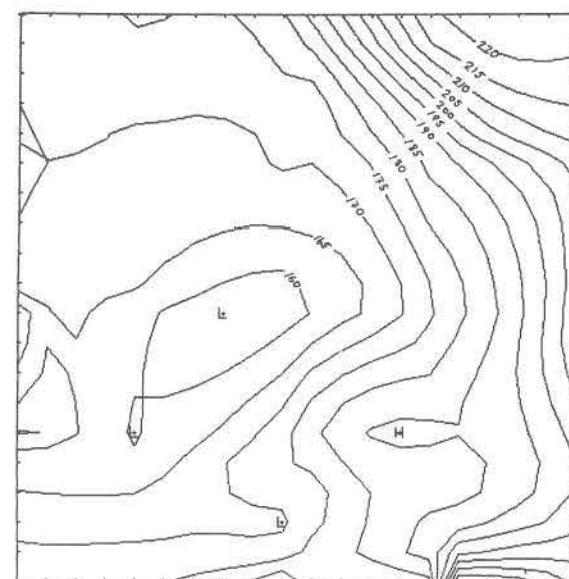
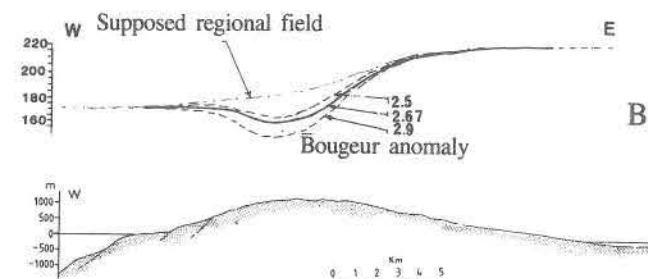
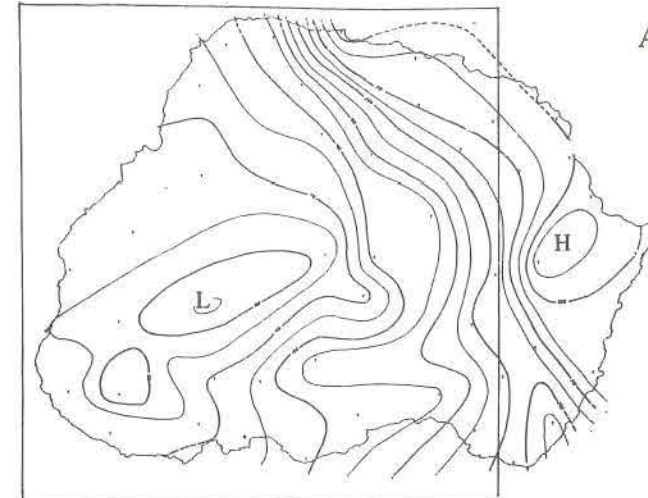
(3%) on the slopes (See Fig 6B). Fig 5 shows clearly an asymmetric pattern with a domain of high values (gravity high) in the east, an area with low values (gravity low) in the west and a marked change between the two. Without gravity observations at sea it is problematic whether or not this pattern can be attributed to the regional field. It is, however, worth noting the parallelism between the asymmetrical shapes of both the underlying plateau and an E-W gravity profile as illustrated on the cross-section of Fig 6B. A localised high anomaly appears on the east coast but it is based on only one measurement (station 23) and will not be taken further into account.

Interpretation

The interpretation of the gravity results is hampered by the sparse coverage on the island and the absence of gravity measurements at sea as can be seen on Fig 6A. These values were gridded using an inverse square gridding algorithm (Davis 1973) and the contoured Bouguer anomaly values are shown in Fig 6C. The gridding algorithm used created data by polynomial extrapolation for very limited areas surrounding the island out in the sea. To isolate

Fig 6: Calculation of the residual gravity anomaly.

- A — The sector of interest for which residual anomaly and gravity modelling were performed avoids the high value on the east coast (gravity assumption of 2.67 g/cm^3)
 B — The general increase of the anomaly from west to east coincides with the topography of the substratum: deep sea floor to the west and submarine plateau to the east. This increase is therefore attributed to the regional field. Compare the Bouguer anomaly profiles for 3 different density assumptions
 C — Gridded and (extrapolated) Bouguer anomaly map of sector delimited on A
 D — Residual anomaly after subtraction of the regional field of the same sector



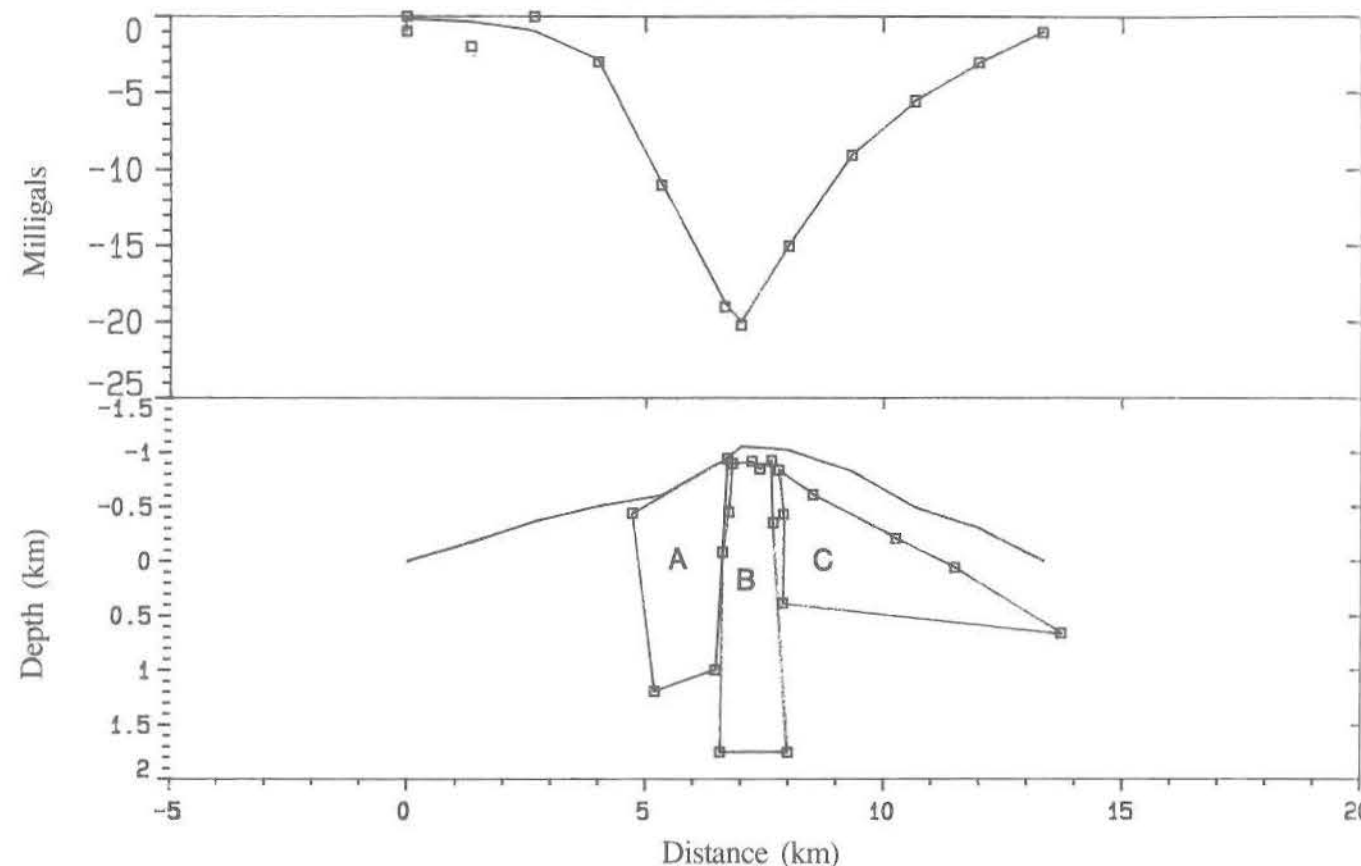


Fig 8: 2D direct modelling of a buried low density body. A and C have a density contrast of -200 kg/m^3 . B has a density contrast of -500 kg/m^3

representing the regional field. Fig 6D shows a strong negative anomaly coinciding with the zone of maximum activity deduced for the volcano (compare Fig 6D with Fig 3).

Negative anomalies are often measured on large silicic volcanic complexes (Rymer & Brown 1986) as a result of a combination of the low density of the magma body at depth and a caldera filled with pyroclastic tuff at surface. On the other hand, positive anomalies are often measured on basaltic volcanoes due to the presence of intrusive complexes at depth (dykes, sills, laccoliths) that are usually more mafic and better consolidated than the surrounding rock. The presence of a strong negative anomaly on the basaltic volcano of Marion does not agree with these general observations.

Using a linear inversion method (Stettler 1980), the extent and density of a body that could be responsible for such a negative anomaly was modelled (Fig 7). The inversion technique uses rectangular building blocks and can build the model upwards or downwards or both from a flat base using the residual gravity field, the density contrast and the depth of the building base as input. For a density contrast of -200 kg/m^3 and a flat building base between 5 and 8 km below surface of the volcano the model produces an unrealistically big and shallow body. A density contrast of -400 kg/m^3 and the base at 6 km give a more satisfactory result but that would mean a basaltic magma of density $2\,200 \text{ kg/m}^3$. Both proposals are unrealistic since the reservoir is supposed to have

reached a level of neutral buoyancy. On the other hand there might be a high concentration of light fluids in the upper part of the volcano just below the most active area or a pile of low-density rocks at shallow depth. Rocks of lower density have been found on the Kilauea volcano at Hawaii (Keller *et al* 1979) for some hundreds of metres, but to create the Marion anomaly a few kilometres of light rocks would be needed. Sub-glacial hyaloclastites were formed on Marion during the Pleistocene period (Verwoerd & Chevallier 1987, Verwoerd 1990). They are well exposed along the coast but their extent inland is unknown. In order to model lateral variation in the volcano, two-dimensional computer-modelling has been done along a profile across the gravity low (see Fig 5 for location). The model technique uses a direct calculus method for two-dimensional bodies with an infinitely long third dimension. The result shows that, in order to produce the observed anomaly, a body of 2.5 km in vertical extent and with a density contrast of -500 kg/m^3 is needed in addition to a gravity contrast of -200 kg/m^3 on the flank of the volcano (Fig 8). The negative anomaly on Marion must therefore be regarded as exaggerated. Possible reasons for this could include the following:

A — Altitude error. The negative anomaly on Marion is not localised but is a general feature based on numerous stations. If the negative anomaly is due to altitude error it would mean that the error is always in the same direction (always too high) and continuously increases

toward the top of the island. This seems improbable. In addition, for a density of $2\,670 \text{ kg/m}^3$ the Bouguer anomaly would change in the region of two gravity units (0.2 mgal) per metre. If the error of the barometrically determined heights are in the order of ± 10 metres the Bouguer anomaly values would change by ± 2 mgal (20 gu). Since the maximum amplitude of the negative residual anomaly is -20 mgal, a ten-metre error would make no difference to the model. The local high value obtained on the east coast (station 23) could possibly be due to altitude error.

B — Wrong density assumption. The Bouguer anomaly was calculated for three density assumptions. The three profiles of fig 6B show that the magnitude of the Bouguer anomaly is significantly affected at the top of the volcano but the shape of the profiles remain the same. In order to annul the negative anomaly a very low density assumption would have to be made.

C — Terrain correction. No terrain correction, which takes into account the influence of near and far topographic relief, has been calculated. Terrain corrections are always positive. The highest correction would be along the slopes and at the top of the volcano. It is estimated that the maximum terrain effect could be in the region of 5 mgals. This could reduce the negative anomaly somewhat and thereby the calculated size of the body. However a residual anomaly of -15 mgals still needs a body of substantial size to explain such a gravity effect.

D — Wide spacing of stations. This is a problem in gravimetric studies over volcanoes where the grid of observations is not sufficiently close-spaced to resolve short wavelength anomalies. However, on Marion the negative anomaly is not localised; it is indeed a long wavelength anomaly on the scale of the island. The local high anomaly on the east coast is a typical example of a short wavelength anomaly based on insufficient number of stations and the possibility of a local altitude error.

E — Lack of isostatic compensation. The wavelength of the Marion anomaly is too small to be compared with one that would be produced by a volcanic edifice in isostatic disequilibrium.

F — The regional field. In the absence of data, a certain regional field was estimated from coastal measurements. Any other regional field would make quite a difference to the residual anomaly. The real regional field might produce a more positive residual anomaly but there will still be a relative low at the top of the volcano. It is possible that such a residual anomaly could lead to a more realistic model.

Conclusion

The gravity results obtained on Marion are satisfactory despite possible errors due to altitude estimation, terrain correction and density assumption. There is undoubtedly a low gravity anomaly over the most active part of the volcano. However, its amplitude and significance cannot be ascertained without a proper knowledge of the regional

field. Gravity readings are needed at sea before any further conclusions can be reached.

Seismology

A temporary seismological observatory was installed at the meteorological station for a period of four years from May 1987 to May 1991. Technical details of the installation were given by Bova (1988) and the characteristics of the station by Fernandez (1988). The instrument used is a short-period LC4 Mark Products waterproof seismometer with a 1 Hz natural frequency, and calibration coil facilities. It was buried in a waterproof pipe, resting on a concrete base, 5 to 6 metres deep in a Holocene lava flow, some 800 m away from the shore and 20 m south of the Mammal Laboratory (Fig 9). The installa-

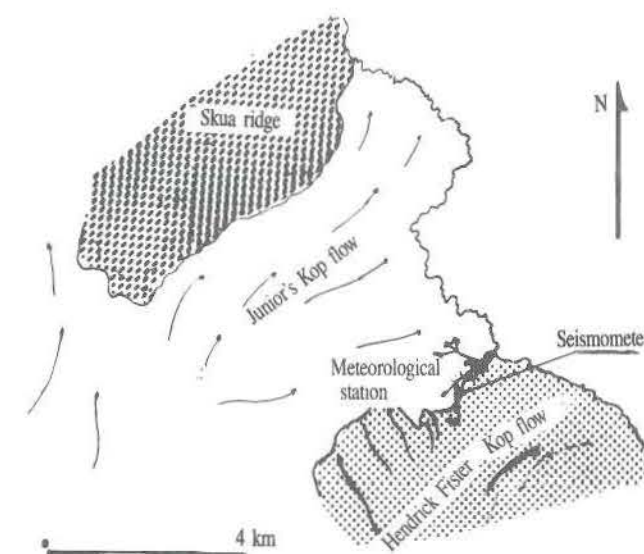


Fig 9: Location of the seismometer at the meteorological station on Marion Island. Arrows indicate lava flow directions

tion was intended to minimise background noise due to sea wave action, strong wind, heavy rain, etc. Despite these precautions, low gain had to be set on the amplifier (6250 magnification at 1 Hz). The recording was done in analogue form on a portable seismograph, RV320B of the Portacorder-type of Geotech, under the control of an operator. The recorder provides electronic amplification of the signal, low and high pass filters and accurate time signals. The corner frequency of the filter was 5 Hz with the low pass filter switched off. The seismograms were sent to the Geological Survey Office in Pretoria for interpretation once a year after each relief voyage.

The purpose of the seismological study was twofold:

— To record the activity of the volcano between eruptions and to seek answers to questions like the following: Is there any sign of magma migration from deep magma storage to higher levels? Is there any stress relaxation inside the edifice?

— To detect any sign of activity before another eruption occurs.

Quality of the records

May 1987 to March 1988 was a test period during which intermittent recordings were made due to technical and operational management problems. Between March and September 1988 the seismograph was brought back for repairs. From August 1988 to May 1991 no major technical problems occurred and continuous recordings were obtained.

The daily records were divided into four categories:

	Good	Fair	Poor	Bad
May 1987 — Mar 1988	121	48	35	56
Sept 1988 — Aug 1989	114	105	67	61
Aug 1989 — May 1990	148	54	25	14
May 1990 — May 1991	175	114	34	17
Total	558	321	161	148

It appears that from September 1988, when the station started operating efficiently on a daily basis, 75% of the records are good to fair. Examples of good, fair, poor and bad records were given by Fernandez (1988) who reported on the performance of the station for the period May 1987 to March 1988.

Recording of seismic activity

The earthquakes recorded at Marion station fall under three categories: teleseisms, regional earthquakes and local events.

Teleseisms

These are by far the most commonly recorded earthquakes but are irrelevant to the problem. They are characterised by relatively longer period waves (Fig 10) and have been identified and localised by the National Earthquake Information Centre (NEIC) of the United States Geological Survey.

Regional earthquakes

These events are less numerous; seven have been recorded in four years (Fig 11). The S-P wave time difference is between 20 and 30 seconds, indicating epicentral distances of about 300 km. These recordings are the result of typical tectonic events originating on the South Indi-

an Ridge (Fig 12). Two of them, of magnitude greater than 4.5, have been registered and located by NEIC. However, due to poor coverage in this part of the globe it is estimated that the location is only accurate to within 50 km.

Local events

Four local events were recorded in three years (Fig 13). They are of very small magnitude and lasted for 10 to 30 seconds. P and S wave signals are very close together, indicating a hypocentre located within 10 km. Their interpretation is rather difficult with the limited data at disposal. Volcanoes exhibit seismicity due to rock-fracturing (tectonic or dyke propagation related), magma movement, or combinations of these (Klein *et al* 1987). On Fig 14 are given examples of volcanic earthquakes recorded on two active and continuously monitored oceanic volcanoes. The first example is from Piton de la Fournaise volcano on Reunion Island (Bachelery *et al* 1982). The earthquake, which lasted 5 minutes, occurred four weeks before an eruption. The S phase was followed by low frequencies and P wave polarities varied from station to station. It was interpreted to be the result of the movement of magma at a depth of 10 to 15 km without fracturing. The second example shows a series of short-period earthquakes interpreted to be due to fracturing and dyke propagation a few days before an eruption on Kilauea, Hawaii (Koyanagi *et al* 1987). The signatures are very different from the Reunion example: a multitude of short events, with high initial frequencies, quick attenuation and close proximity to the surface.

The four local seisms on Marion do not appear to be related to dyke propagation; their signatures are similar to those of events due to fluid (magma or gas) movement. They could also be due to isolated small tectonic fractures resulting from local readjustment of the volcanic pile during a rest period.

It is concluded that the seismicity of Marion and Prince Edward Islands is very low. The level of seismicity of an oceanic volcano between eruptions varies from one edifice to another. For instance, there is a sharp difference between the two examples cited above (Kilauea and Piton de la Fournaise). At Kilauea (Fig 15) each period of rest between eruptions is characterised by a high level of seismicity with the monthly number of events of mag-

Malawi - 11/03/1989 - 34.04E 12.20S - Mag 6.2

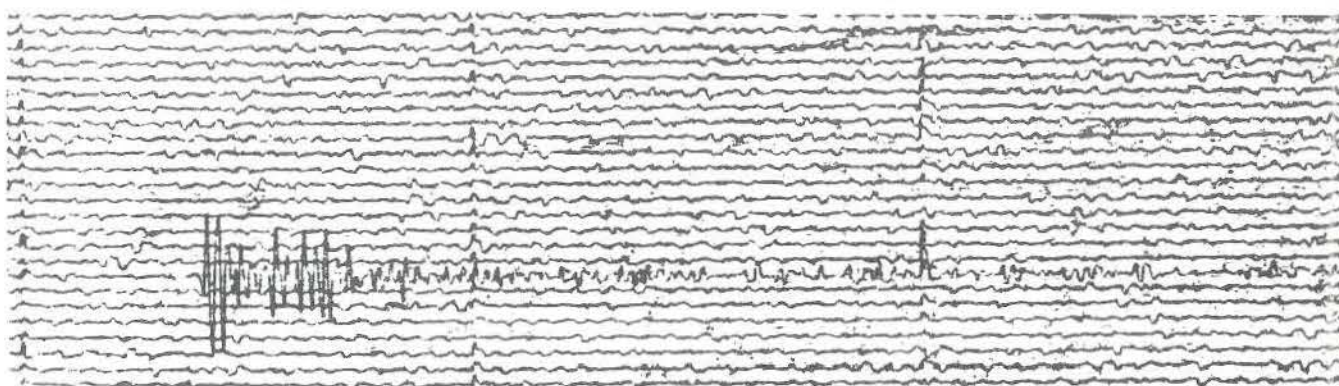
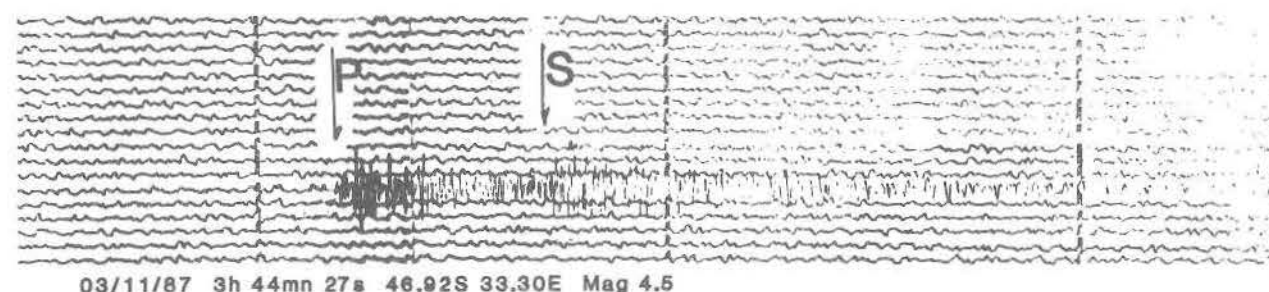
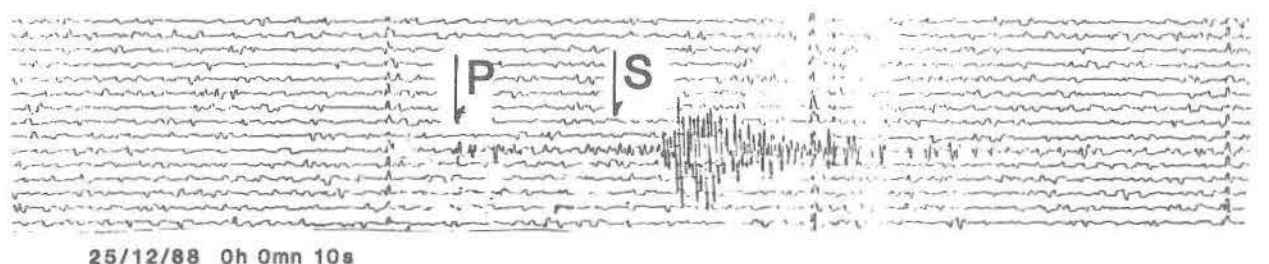


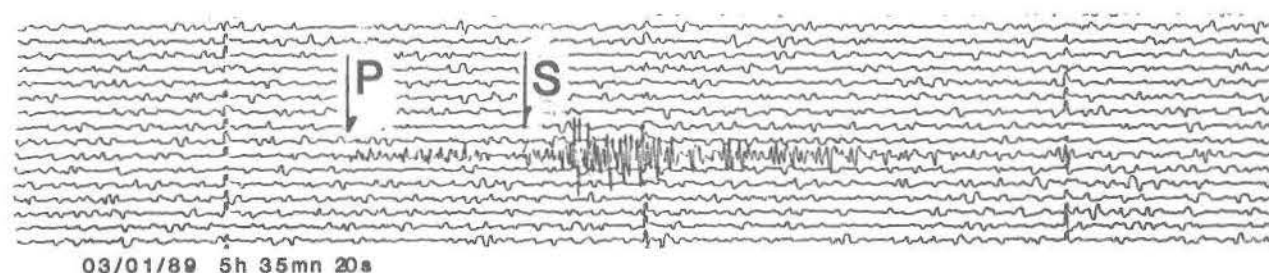
Fig 10: Example of a teleseism



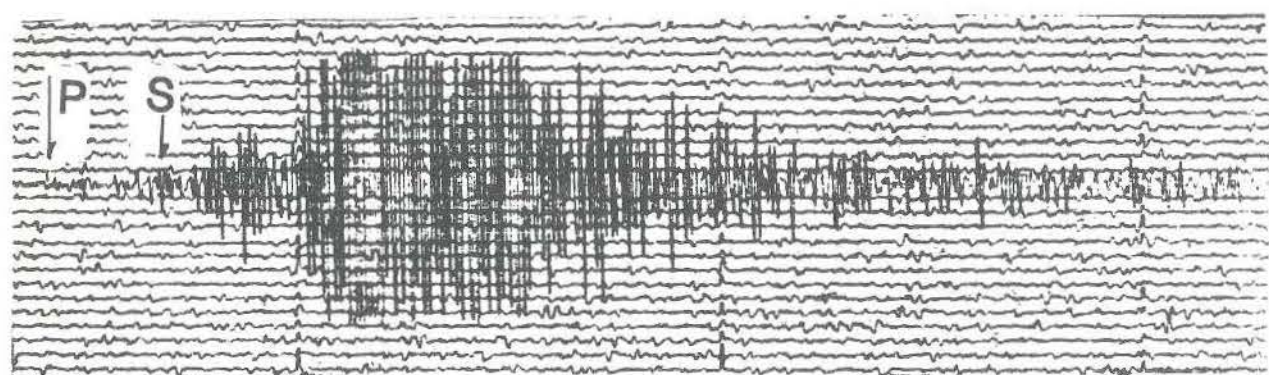
03/11/87 3h 44mn 27s 46.92S 33.30E Mag 4.5



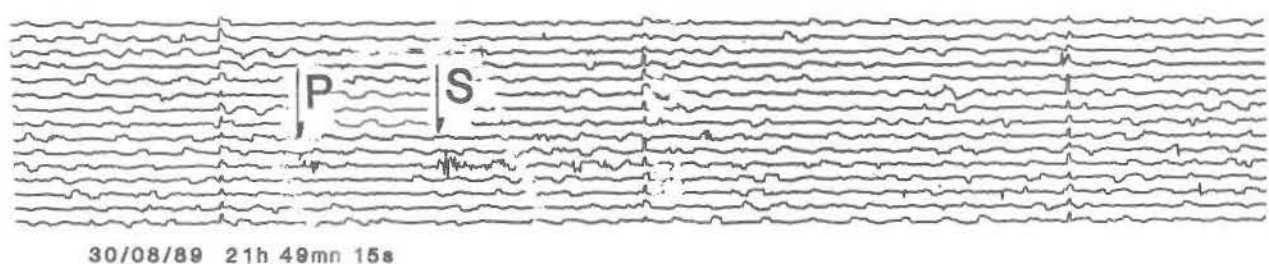
25/12/88 0h 0mn 10s



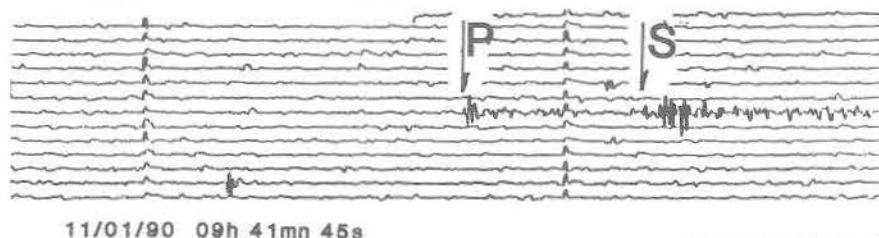
03/01/89 5h 35mn 20s



13/06/89 23h 0mn 25s 43.39S 38.67E Mag 5.1



30/08/89 21h 49mn 15s



11/01/90 09h 41mn 45s



4/03/1991 06h 44mn 10s

Fig 11: Examples of regional seisms. They all originate in the mid-ocean ridge area of the SE Indian Ocean (see Fig 12)

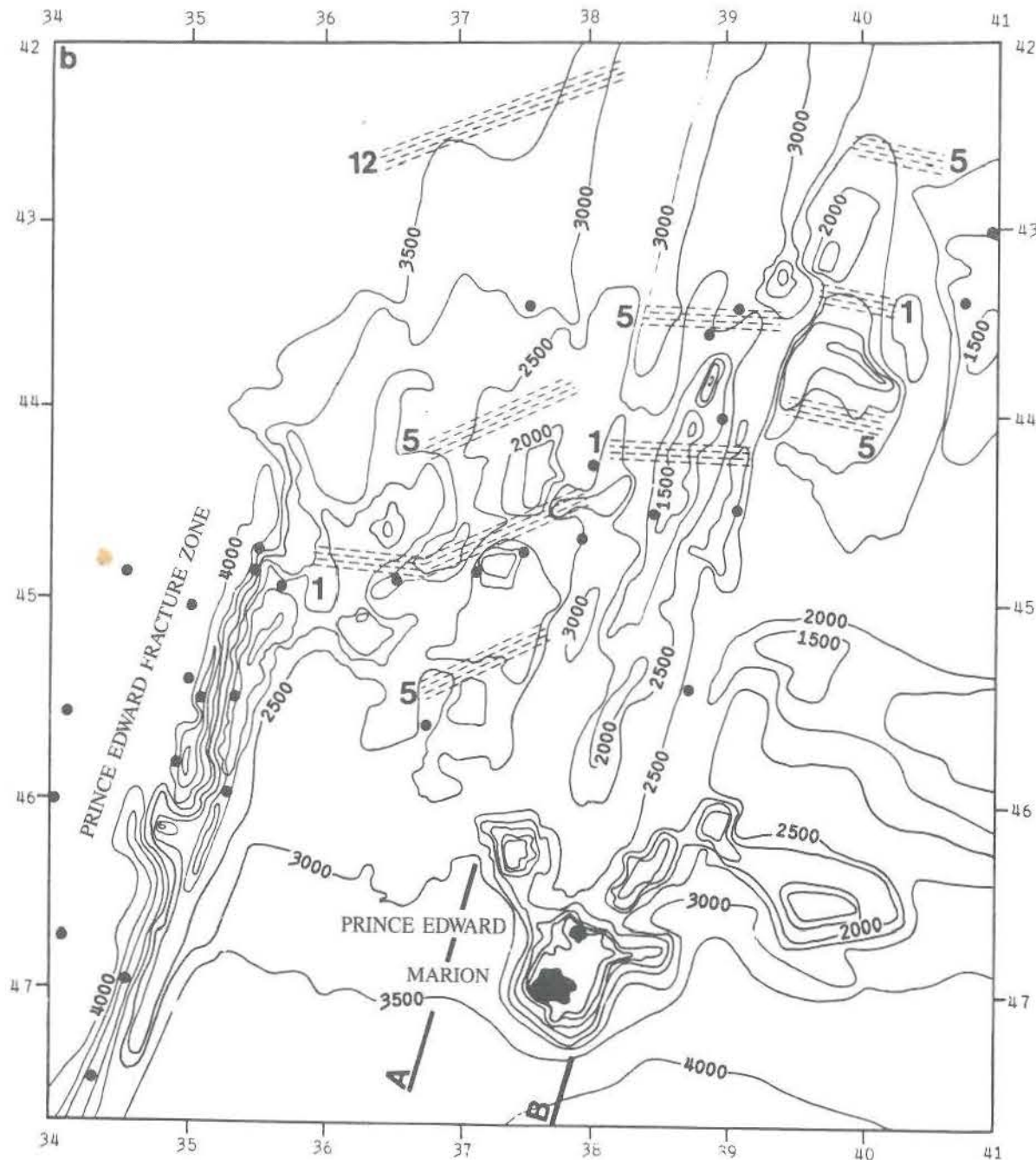


Fig 12: Location of regional seisms recorded during the last ten years. Dots: epicentres. Number 1, 5, 12: Sea floor magnetic anomalies (after Bergh & Norton 1976). Other numbers are isobaths. A and B: Fracture zones

nitide >1 exceeding 100 (Klein *et al* 1987). At Reunion only a few events have been recorded in the five months preceding the 1983 eruption (Fig 16, Lenat *et al* 1989). At both volcanoes seismicity increases drastically one or two weeks before the eruption.

Conclusion

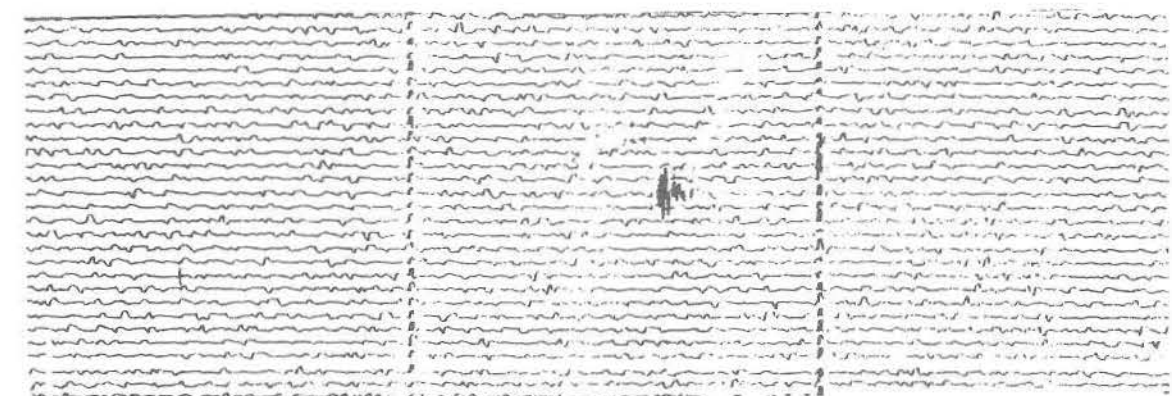
Owing to severe weather conditions on Marion Island the seismic station did not operate at its optimum. Of the records 75% were of good to fair quality. In addition the amplification power of the seismograph was very limited. Only a magnification of 6 250 for harmonic waves of 1 Hz was applied. This low gain imposed serious restrictions on the number of earthquakes recorded.

Despite these problems it seems clear that Marion Is-

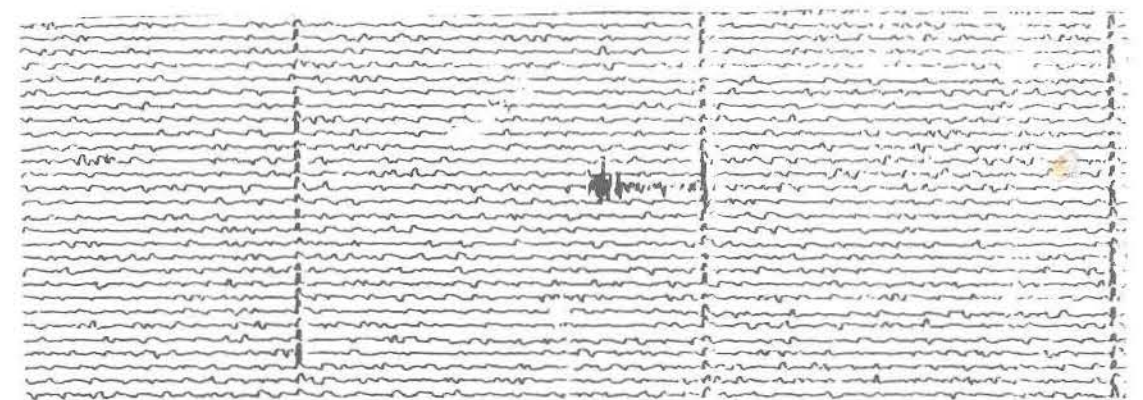
land has had a low level of seismicity during the four-year testing period. Deep magma movements or elastic readjustment may have been recorded but no sign of shallow fracturing or dyke propagation was detected. Seismological observations on Marion should be undertaken on a routine basis and would be of great value to knowledge of Marion volcano dynamics if another eruption ever occurs.

Ground magnetic profiles

A preliminary ground magnetic survey was conducted during the August 1987 and August 1988 expeditions to Marion in order to test the magnetic response of the different geological formations and the feasibility of a



19/01/88 21h 44mn 35s



20/01/88 21h 53mn 40s



29 04/89 23h 5mn 30s



7/08/90 05h 25mn 10s

Fig 13: Local seisms. Note that P and S wave signals are close together

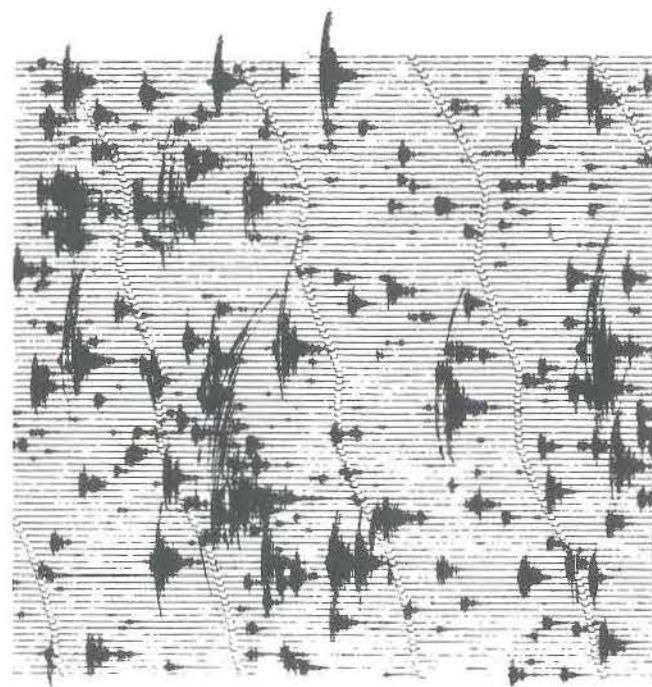
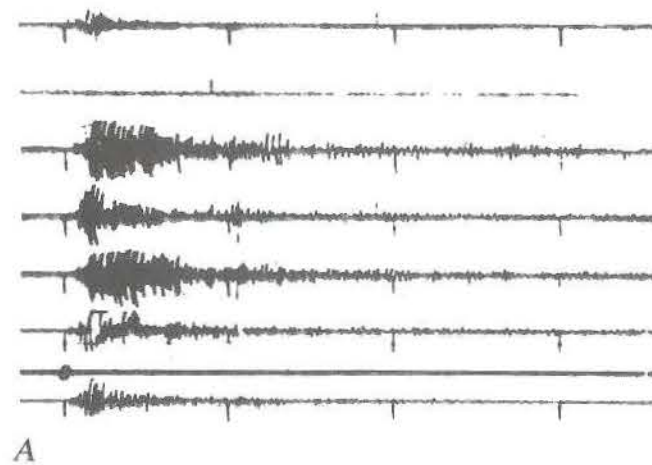
future airborne survey. Two portable instruments were used, a Geometric proton magnetometer and a flux gate magnetometer.

The magnetic field

A permanent geomagnetic station was installed on Marion from 1973 to 1980 by the Magnetic Observatory of the

CSIR (CSIR reports Mag F1, F2, F3, F4, F5). The main annual field value decreased from 33 965 nT in 1973 to 33 425 nT in 1980. Variations of the declination and horizontal and vertical fields are given in report Mag F5.

For calibration, a Varian proton magnetometer (generally used for marine geomagnetic purposes) was installed at the meteorological station and remained there for the



B

Fig 14: Examples of volcanic earthquakes recorded before an eruption

A — Piton de la Fournaise (Bachelery et al 1982). The same event recorded at different stations. It has been interpreted to be related to deep magma movements a few weeks before the eruption

B — Hawaii (Koyanagi et al 1987). Dyke propagation event signatures recorded at one station a few days before the eruption

duration of the 1987 expedition. The sensor was hung on an aluminium tripod, 1 m above the ground, and some 200 m from the radio antenna. The recording was very steady (a few nanotesla variation). The continuous background varied between 32 810 and 32 890 nT over a period of two hours.

The profiles

Readings were taken on four profiles selected in such a way that different geological formations and features were traversed: Pleistocene lava flows, moraines, Holocene flows, a fault and a magma-intruded fracture (Fig 17).

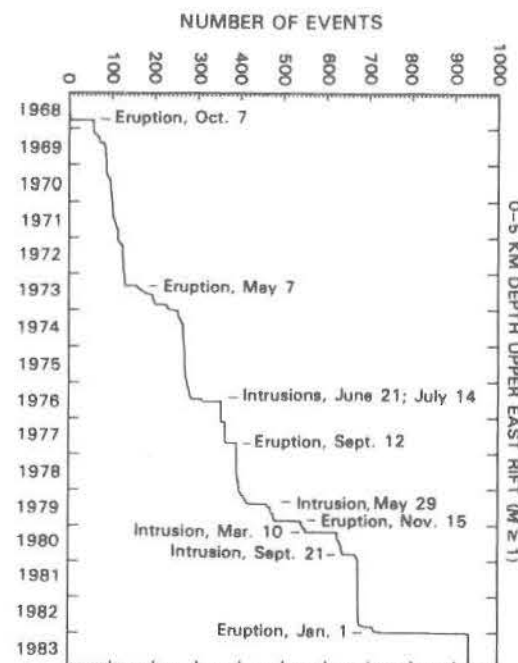


Fig 15: Frequency of earthquakes before eruption on Hawaii (Klein et al 1987)

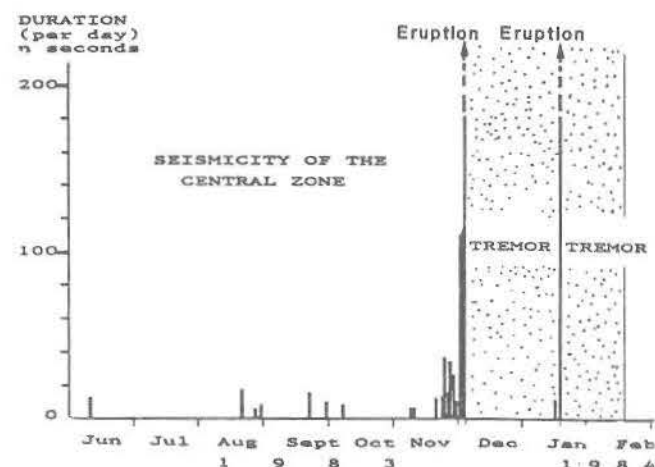


Fig 16: Frequency of earthquakes before eruption on Piton de la Fournaise (Lenat et al 1989)

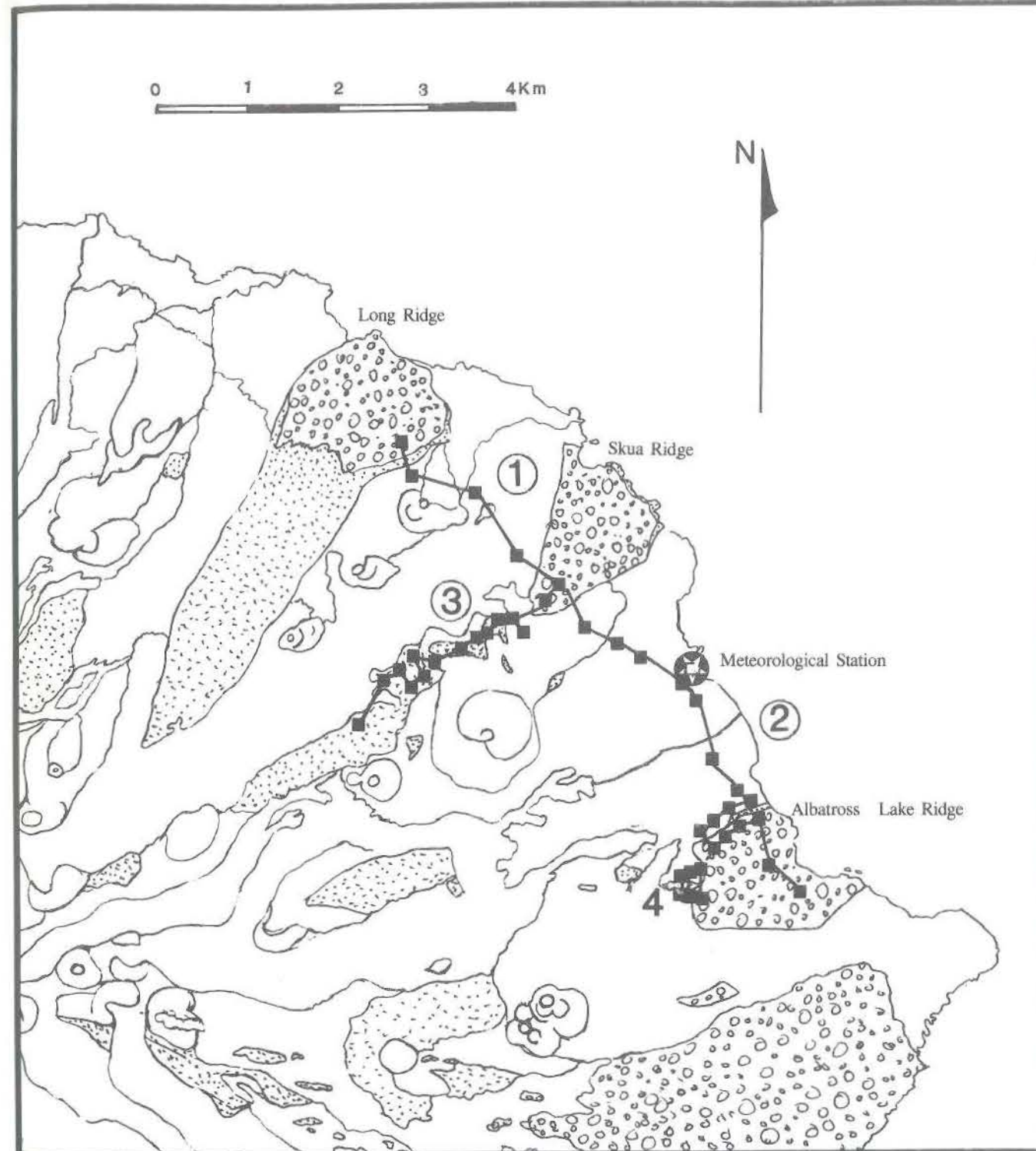


Fig 17: Location of ground magnetic profiles

The first profile runs from the meteorological station north-westward to Long Ridge and crosses Holocene lavas and moraines alternately.

The second profile runs from the same starting point to Albatross Lake Ridge across Holocene flows and a fault that brings moraine-covered Pleistocene flows in contact with Holocene flows. The third profile follows

a single geological formation: a series of Pleistocene lavas composed of about ten massive flows.

The fourth profile (a series of three parallel sub-profiles) crosses an E-W linear chain of small Holocene eruptive cinder cones. These are characteristic of a fissure eruption and a feeding dyke must be present at shallow depth.

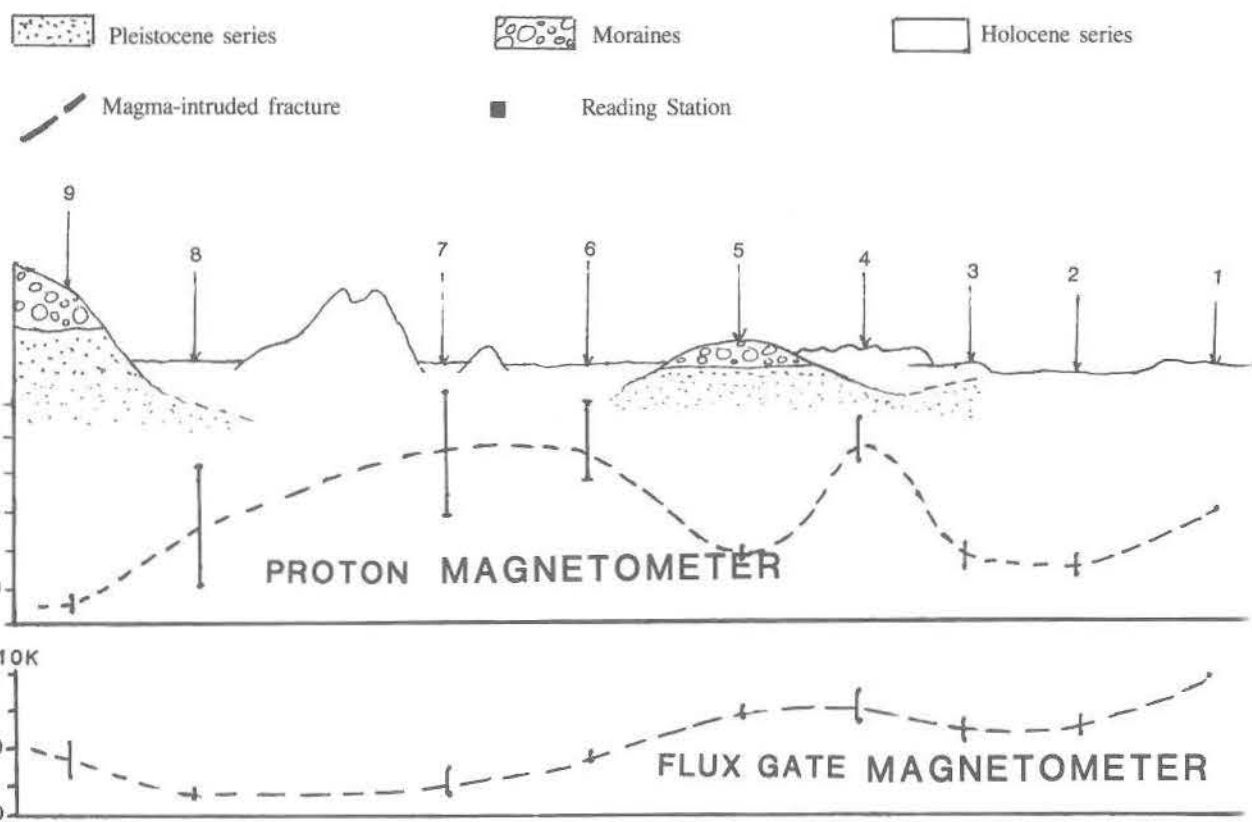
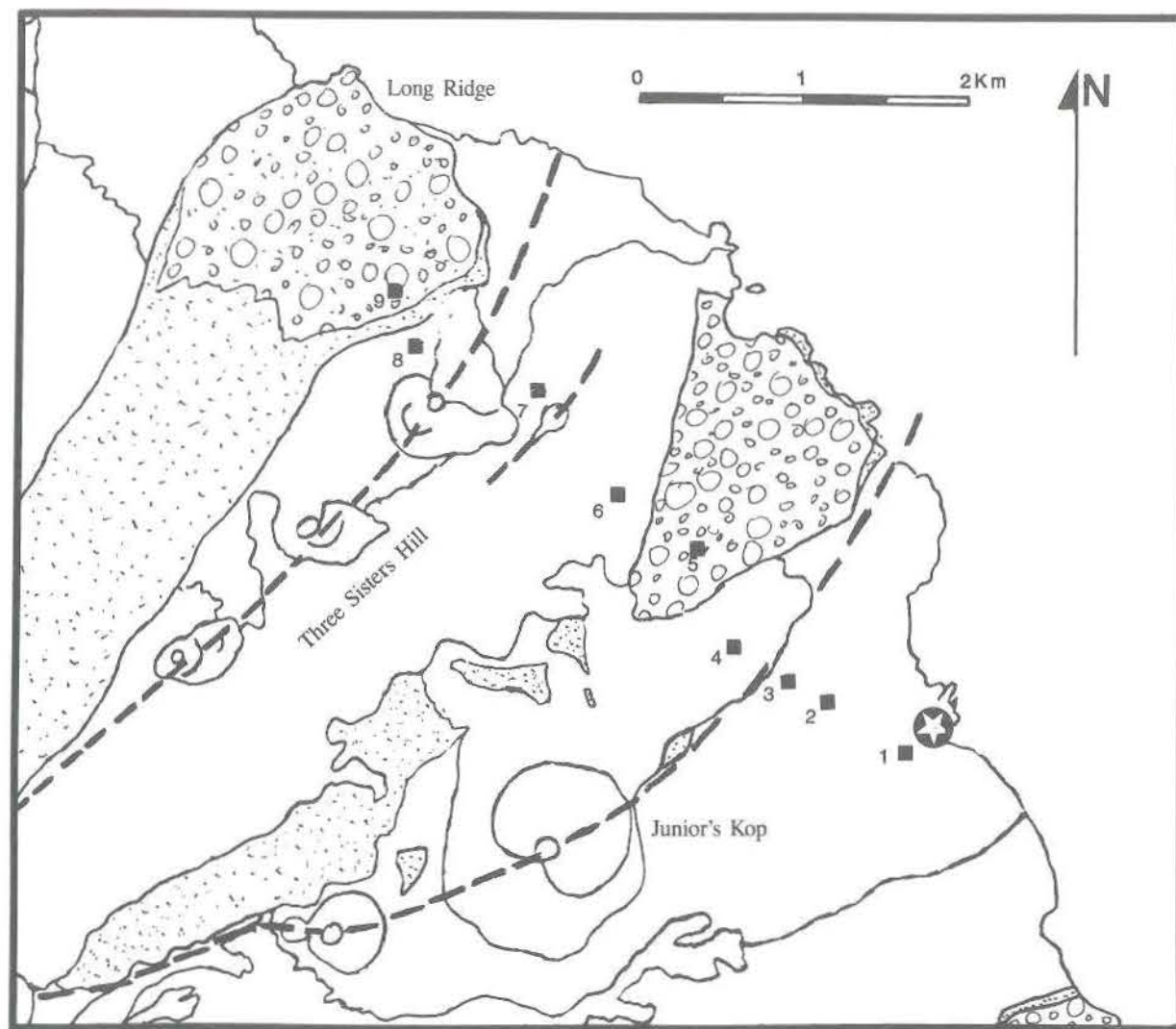


Fig 18: Profile No 1. Note low and consistent values above moraine-covered Pleistocene lavas on the proton magnetometer, and the opposite effect on the flux gate magnetometer

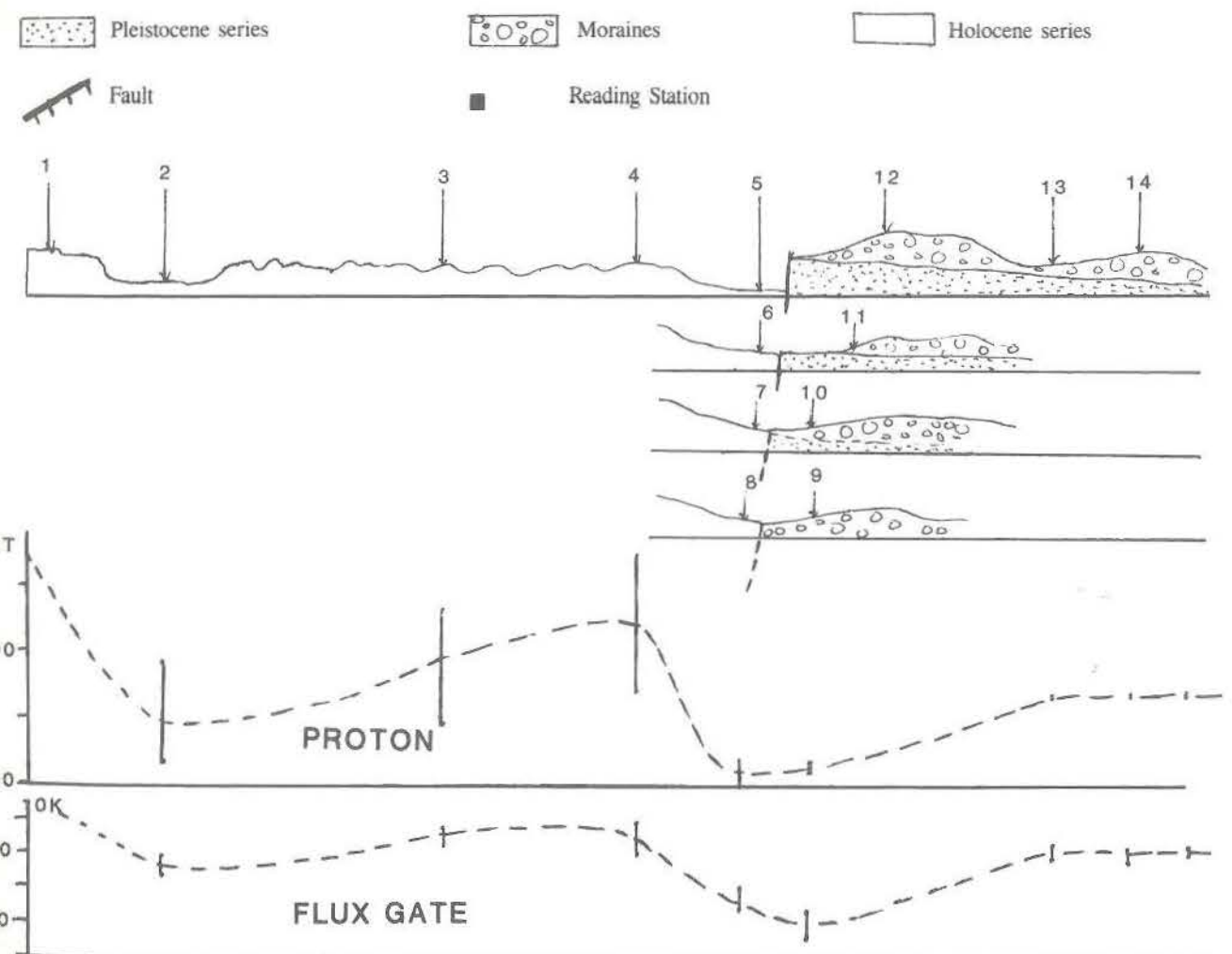
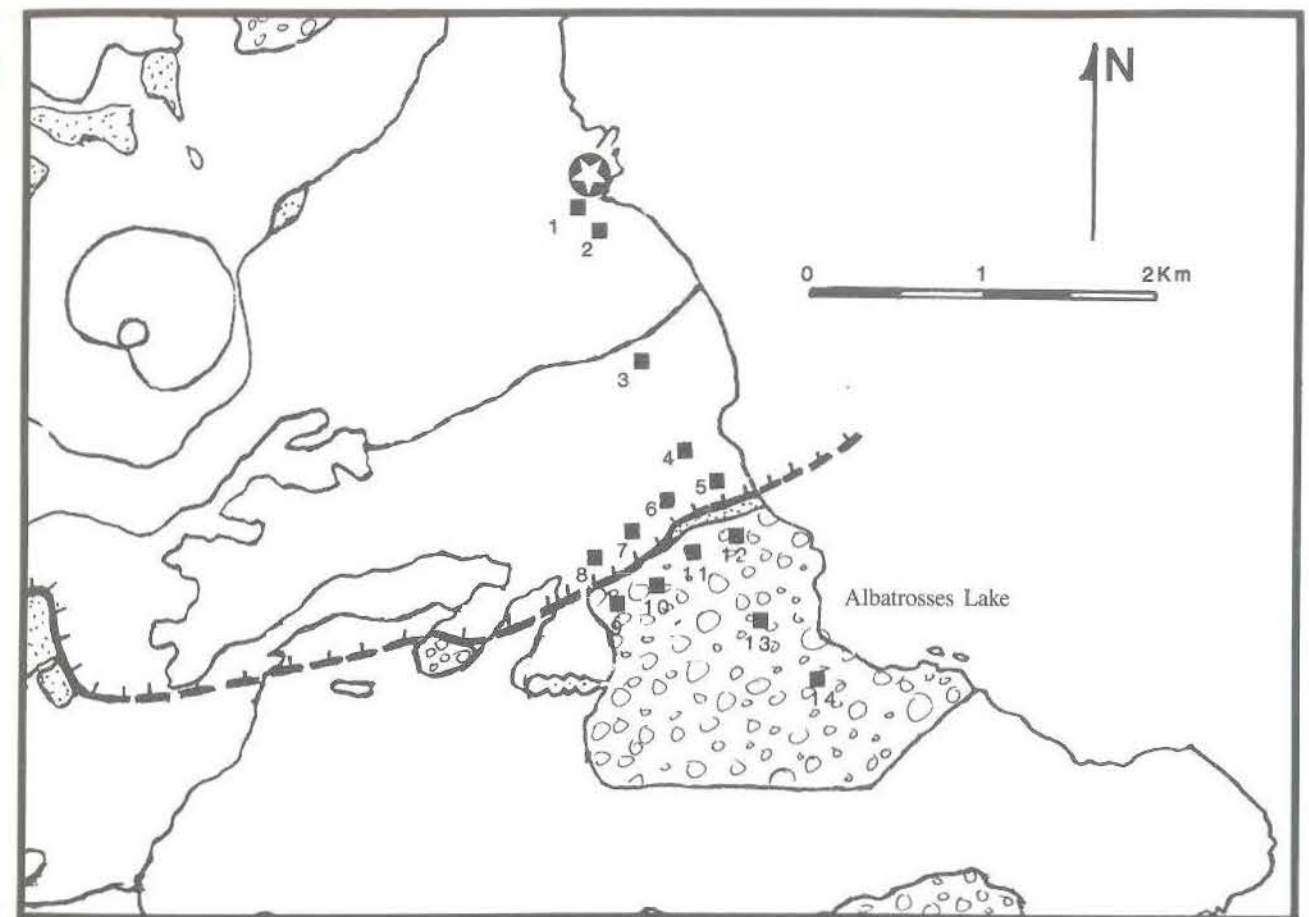


Fig 19: Profile No 2. Note the sharp contrast at the contact between Holocene flows and the Pleistocene moraines

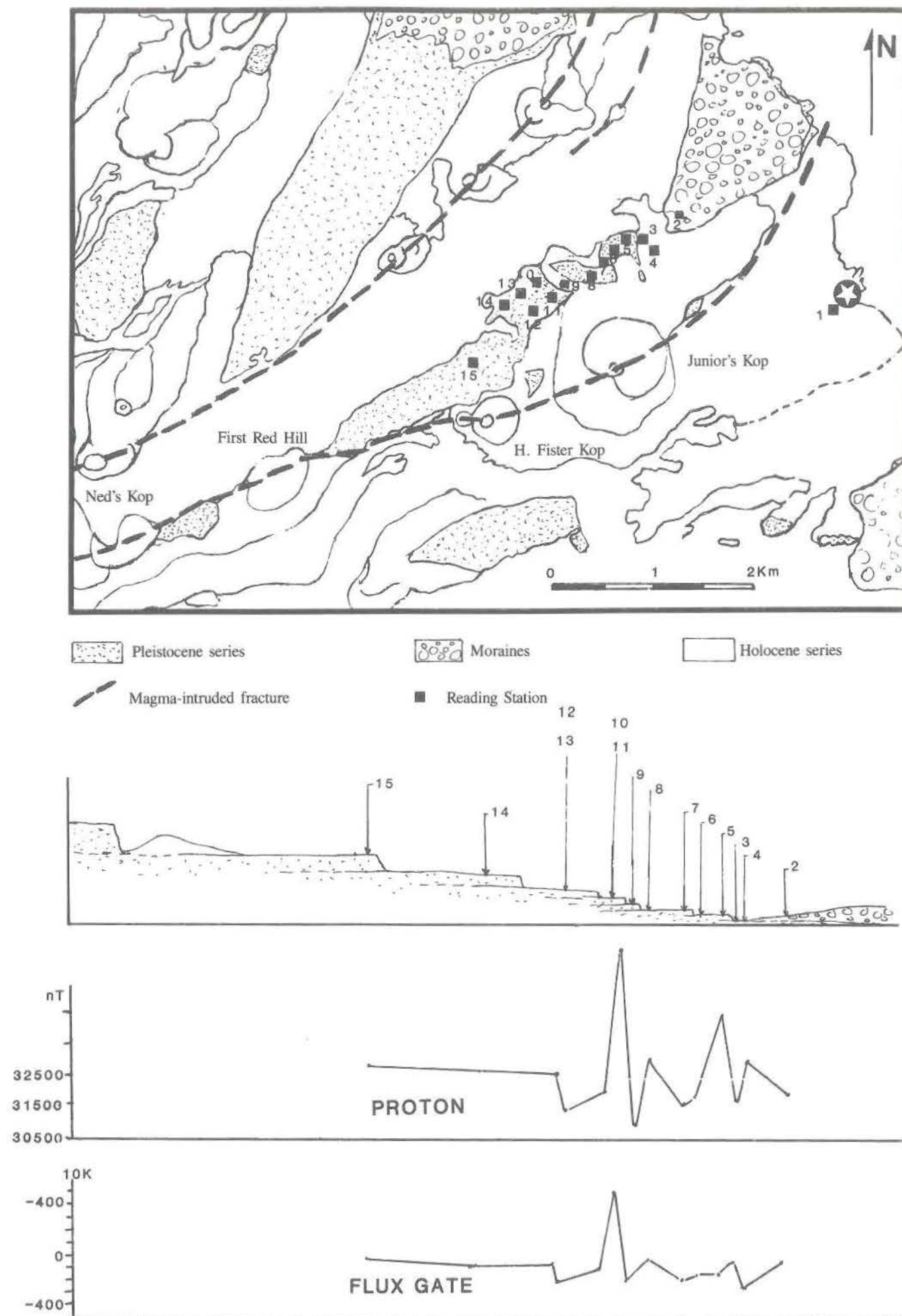


Fig 20: Profile No 3. Note the constant average value but the inconsistent readings

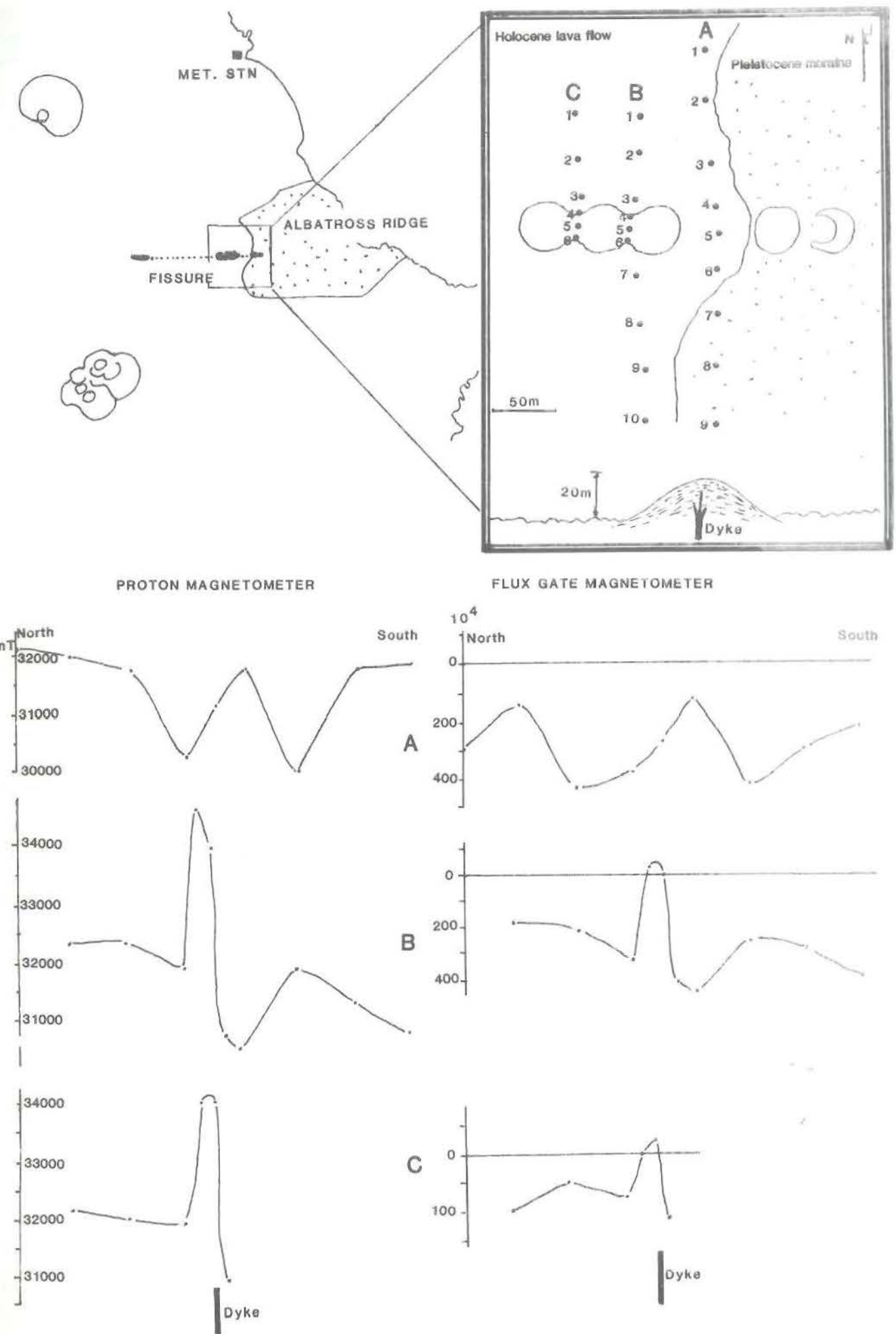


Fig 21: Profile No 4. The effect of the dyke is well marked in all three traverses on both magnetometers

Results

Profile No 1

The average spacing between the stations was 500 m (Fig 18). Measurements were also taken offset 100 to 200 m of each station in order to test the steadiness of the magnetic field over a specific area and the validity of the reading.

On the proton magnetometer curve high values were obtained over the Holocene flows with lateral variability in the readings (vertical error bars) whereas lower values and laterally more consistent readings were observed over the moraine and Pleistocene formations. If this pattern is reliable, Holocene lava appears to be very thin at stations 2 and 3.

The flux gate magnetometer curve (that shows only the vertical field) in general shows an opposite pattern with high readings over Pleistocene and low over Holocene formations, but without sharp gradients. Compared to other profiles this behaviour does not seem to be right and the result should be disregarded.

Profile No 2

The average spacing between the stations was similar and readings were also taken at different places around the stations (Fig 19).

Proton and flux gate magnetometer curves show similar patterns with high and inconsistent values over the Holocene flows, a sharp drop at the contact with the Pleistocene flows and very steady lower values over the moraines. The fault and the contact Pleistocene-Holocene have a marked effect on the magnetic profiles.

Profile No 3

The stations were more closely spaced (around 200 m). Proton and flux gate curves are similar (Fig 20). The Pleistocene flows show a constant average reading but strong lateral variations.

Profile No 4

On this profile the stations were closely spaced in order to detect the shape of the magnetic anomaly above the supposed dyke (Fig 21). The results show a magnetic anomaly characteristic of a shallow dyke and is very well marked above the fissure. For each profile both proton and flux gate curves give the anomaly shape. Modelling have shown that the differences between profile A and profiles B, C could be attributed to bifurcation of the dyke.

Conclusion

The geophysical results support a few important points already deduced from the geology.

The shallow magma chambers under the volcano and the elongated zone of volcanic activity at surface correspond to a gravity low. However, the nature and the amplitude of the anomaly is not accurately known due firstly to lack of knowledge about the regional gravity field and secondly due to the paucity of gravity stations.

The low rate of eruption of the volcano and the ongoing

petrological differentiation in the chamber coincide with a period of relative seismic quietness. However, some deep magma movements might occur that could lead to magma chamber replenishment.

Ground magnetic surveys hold promise for detecting shallow feeder dykes on a local scale but are certainly not appropriate to the large scale of the island as a whole. The magnetic survey was carried out on the least volcanically active part of the island but still showed extreme variability. An aerial magnetic survey above the most active zones of the volcano would not only give more efficient coverage but will eliminate much of the erratic variation associated with ground surveys and may reveal major feeding channels and tectonic fracturing.

Acknowledgements

The research was supported by the Department of Environment Affairs on a SASCAR programme under the aegis of the Foundation for Research Development and by the Geological Survey of South Africa.

References

- BACHELERY P, BLUM PA, CHEMINEE JL, CHEVALLIER L, GAULON R, GIRARDIN N, JAUPART C, LALANNE F, LE MOUËL JL, RUEGG JC & VINCENT P 1982. Eruption at Le Piton de la Fournaise volcano on 3 February 1981. *Nature* 297: 395-397
- BERGH HW & NORTON IO 1976. Prince Edward Fracture Zone and the evolution of the Mozambique Basin. *J. Geophys. Res.* 81: 5221-5239
- BOVA P 1988. Installation of a seismological station at Marion Island. April 1987. *Geological Survey of South Africa*, report no 1988-0162, 17 pp plus seismograms
- CHEVALLIER L 1986. Tectonics of Marion and Prince Edward volcanoes (Indian Ocean): result of regional control and edifice dynamics. *Tectonophysics* 124: 155-175
- CHEVALLIER L, MC DOUGALL I & VERWOERD WJ (in prep). Constructional stages of Marion Island volcano, Southern Indian Ocean
- CHEVALLIER L & VERWOERD WJ 1988. A numerical model for the mechanical behaviour of intraplate volcanoes. *Jnl. Geophys. Res.* 93: 4182-4198
- CHEVALLIER L & VERWOERD WJ (in prep). Petrology of Marion Island Volcano. Dynamics of magma reservoirs and characteristics of the source
- CSIR report Mag F1, F2, F3, F4, F5. Magnetic observation at Marion 1973-1974, 1975, 1976, 1977, 1978-1980
- DAVIS CD 1973. *Statistics and data analysis in geology*. John Wiley and Sons, Toronto. pp 550
- DU PLESSIS JG 1984. Regionale Gravitatie Opname van die 2330 (Tzaneen) 1:250 000 vel. *Rep. geol. Surv. S. Afr.* (Oop lêerverslag)
- DU PLESSIS JG & BOVA P 1989. Regional gravity survey, Marion Island. *Geological Survey of South Africa*, Report 1989-0047, 6 pp plus 2 maps
- FERNANDEZ LM 1988. An analysis of the performance of the seismological station at Marion Island (May 1987 — March 1988). *Geological Survey of South Africa*, Report 1988-1067, 16 pp
- KELLER GV, GROVE LT, MURRAY KC & SHOKAN CK 1979. Results of an experimental drill hole at the summit of Kilauea volcano, Hawaii. *J. Volcanol. Geotherm Res.* 5: 345-385
- KLEIN FW, KOYANAGI Y, NAKATA J & TANIGAWA WR 1987. The seismicity of Kilauea's magma systems. Volcanism in Hawaii, Vol 2, eds RW Decker, TL Wright & P Stauffer, *US Geological Survey Prof. Pap.* 1350: 1019-1186
- KOYANAGI RY, CHOUET B & AKI K 1987. Origin of volcanic tremor in Hawaii, Part I: Data from Hawaiian Volcano Observa-

- tory 1969-1985. Volcanism in Hawaii, eds RW Decker, TL Wright & P Stauffer. *U.S. Geological Survey Prof. Pap.* 2: 1350
- LENAT JF, BACHELERY P, TARITS P, CHEMINEE JL & DELORME H 1989. The December 4, 1983 to February 18, 1984 eruption of Piton de la Fournaise (La Reunion, Indian Ocean): description and interpretations. *J. Volcanol. Geotherm Res.* 30: 87-112
- RYMER H & BROWN GC 1986. Gravity fields and the interpretation of volcanic structures: geological discrimination and temporal evolution. *J. Volcanol. Geotherm Res.* 27: 229-254
- SEARS WS, SEMANSKY MW & YOUNG HD 1976. *University Physics*. 5th Edition. Addison-Wesley Publishing Co Inc
- STETTLER EH 1980. A geophysical and geological investigation into the diamondiferous gravel runs on Ruigtelaagte, Lichtenburg District. Unpublished MSc thesis. Univ Pretoria, 210 pp
- VERWOERD WJ 1971. Geology. In: *Marion and Prince Edward islands*, eds EM van Zinderen Bakker, JM Winterbottom & RA Dreyer. AA Balkema, Cape Town. 40-62 pp
- VERWOERD WJ 1990. Marion Island. In: *Volcanoes of the Antarctic Plate and Southern Oceans*, eds WE Le Masurier & JN Thomson. *Am. Geophys. Union. Antarctic Research Series* 48: 411-420
- VERWOERD WJ & CHEVALLIER L 1987. Contrasting types of surtseyan tuff cones on Marion and Prince Edward Islands, Southwest Indian Ocean. *Bull. Volcanol.* 49: 399-417
- VERWOERD WJ, RUSSELL S & BERRUTI A 1981. 1980 volcanic eruption on Marion Island. *Earth Planet. Sci. Lett.* 54: 153-156
- WIID BL 1961. Gravity observations at Marion Island, Tristan da Cunha and Gough Island. *Trans. roy. Soc. S. Afr.* 36 (3): 119-128
- WIID BL & VAN WYK AM 1961. Geomagnetic observation on Marion Island, Gough Island and Tristan da Cunha. *Trans. roy. Soc. S. Afr.* 36 (2): 107-117